

Seismic coupling of shallow continental faults and its impact on seismic hazard in Italy



Michele M. C. Carafa
INGV, L'Aquila
michele.carafa@ingv.it

Vanja Kastelic
INGV, L'Aquila

Peter Bird
University of California, Los Angeles

Luca Valensise
INGV, Roma



In the most earthquake-prone areas of the world, including Italy, fault-based seismic hazard is slowly but steadily replacing – or at least complementing – the seismicity-based or zone-based approaches used in the past (e.g. Stucchi et al. 2011). The core of these largely empirical-statistical applications is the projection into the future of historical seismicity as generated by “seismic zones”, finite areas each point of which is presumed to have the same probability of releasing earthquakes following a specific magnitude-frequency distribution. The main drawback of such applications rests in the often short and spatially-incomplete record of earthquake occurrence, which fails to adequately sample the long-term average of seismic release. A comparison of the characteristic length of the earthquake record conducted for Italy (Stucchi et al. 2004), a country that features an especially long seismic history, with the expected long-term slip rate for local faults (Valensise & Pantosti 2001a; Basili et al. 2008) suggests that the activity of two out of three sources of potentially damaging events (Mw 5.5+) may have gone undetected so far. This implies that not even one complete “seismic cycle” could be represented by the available earthquake sample, let alone that a statistically-sound forecast should encompass at least a few complete “seismic cycles.”

These limitations can be overcome with innovative approaches which use other datasets including fault locations, velocities of benchmarks from geodesy, and azimuths of the most-compressive horizontal principal stress.

How to link Tectonic Moment Rate (\dot{M}_{tect}) to Seismic Moment Rate (\dot{M}_{seis})

$$\dot{M}_{seis} = c \cdot \dot{M}_{tect}$$

seismic coupling
(to be determined)

$$\dot{M}_{seis} = \underbrace{\alpha_0 \cdot M_t^\beta \cdot \Gamma[2-\beta]}_{\text{Historical catalog}} \cdot M_c^{1-\beta} \cdot \exp[M_t/M_c]$$

number of earthquakes above M_t Threshold moment magnitude Corner moment magnitude

$$\dot{M}_{tect} = \mu \cdot A \cdot z \cdot \left(\frac{1}{\sin\theta_1 \cos\theta_1} \cdot \dot{\epsilon}_{med} + \frac{1}{\sin\theta_2 \cos\theta_2} \cdot \dot{\epsilon}_{small} \right)$$

seismogenic thickness
(to be determined)

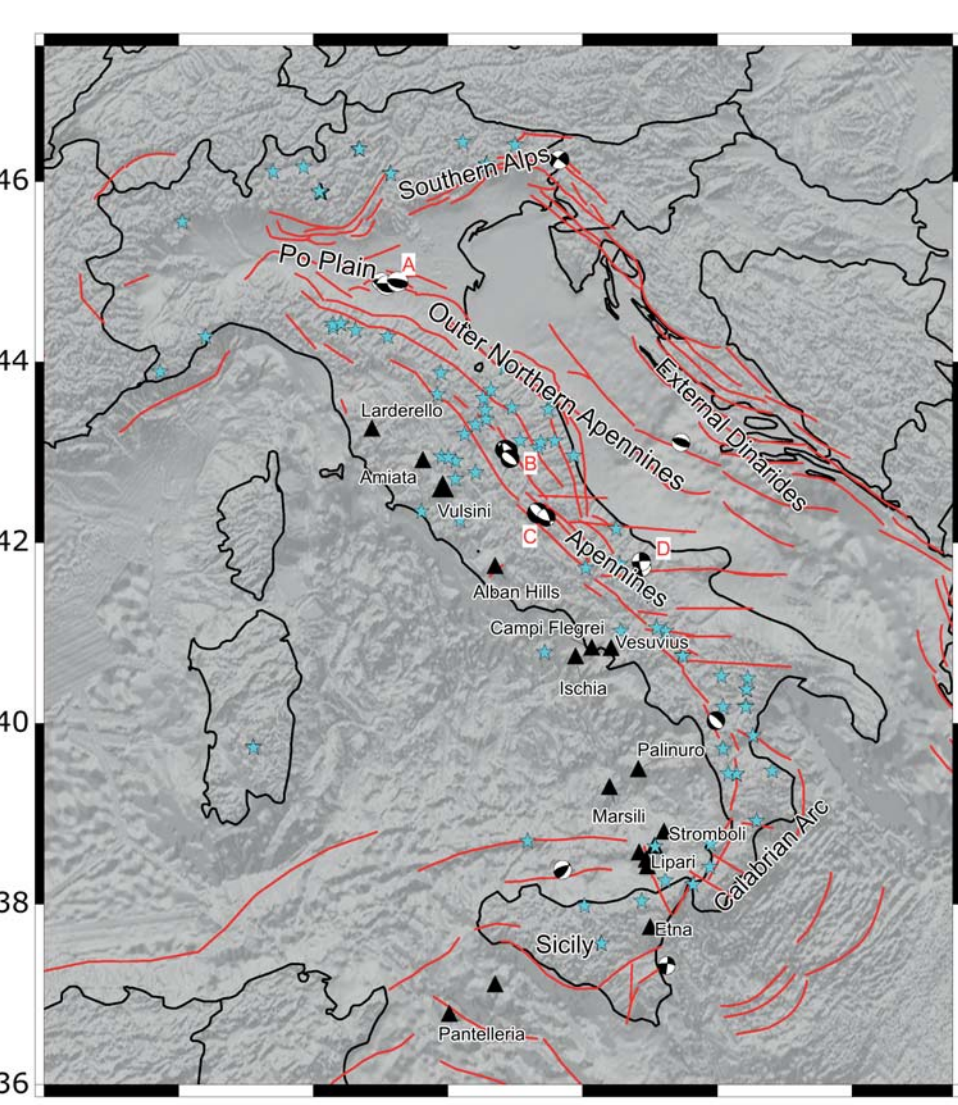
Active fault database + GPS measurements

Thus, to calculate earthquake rates it becomes fundamental the determination of the coupled thickness

$$\langle cz \rangle = \frac{\alpha_0(k) \cdot M_t^\beta \cdot \Gamma[2-\beta] \cdot M_c^{1-\beta} \cdot \exp[M_t/M_c]}{\mu \cdot A \cdot \left(\frac{\dot{\epsilon}_{med}}{\cos(\theta_1)\sin(\theta_1)} + \frac{\dot{\epsilon}_{least}}{\cos(\theta_2)\sin(\theta_2)} \right)}$$

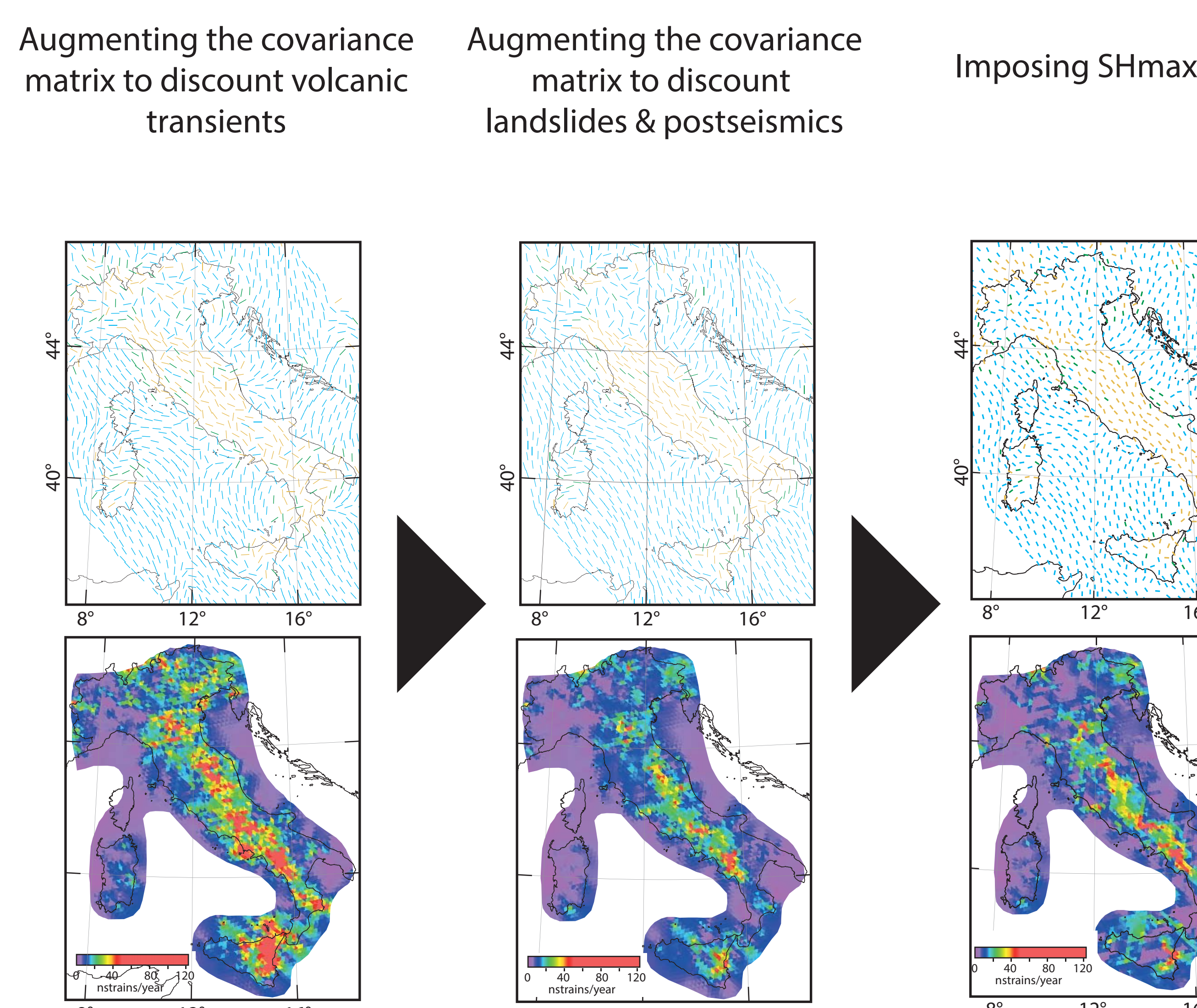
Cleansing GPS dataset to determine long-term strain rates and moment rate

Italy is a country exposed to a number of different short-term transients, including but not limited to landslides, post-seismic relaxation, and volcanic inflation/deflation. These transients infect the GPS velocities and make it difficult the recognition of the tectonic, long-term component of the surface deformation.



★ GPS stations placed < 150 m from active or quiescent landslides
▲ Active or quiescent volcanos

In Bird and Carafa (2016) we elaborated a method for anticipating the principal patterns of non-tectonic, short-term motion and building this information into the covariance matrix of the geodetic velocities. Then, in Carafa and Bird (2016) we applied it to Italy.



The long-term model yields strain rates which may be either elastic, permanent, or mixed because they are based on GPS strain rates whose character is uncertain. The elastic rebound theory, however, suggests that the spatial separation between sites experiencing elastic strain accumulation and non-elastic permanent strain may be as little as a few kilometers or tens of kilometers. Also, it is not practical to attempt to correct observed strain rate fields to an idealized long-term equivalent when dealing with deformation models that do not include faults.

Once we determined the long-term strain rates, we divided the studies area in three regions according to the observed kinematic class:
1. Compressional Faulting Class
2. Extensional Faulting Class
3. Strike-slip Faulting Class

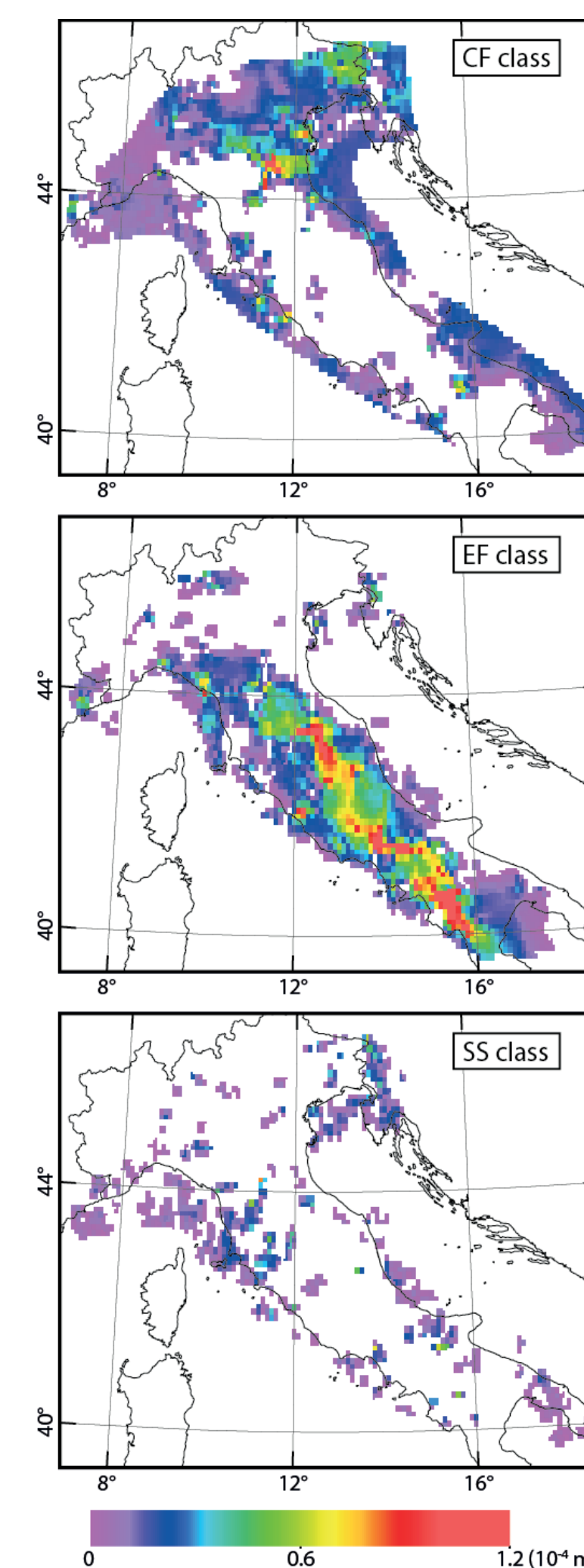
For each one of these classes we can determine the diffusivity D of the deforming volume of the lithosphere

$$D = A \cdot \left(\frac{\dot{\epsilon}_{med}}{\cos(\theta_1)\sin(\theta_1)} + \frac{\dot{\epsilon}_{least}}{\cos(\theta_2)\sin(\theta_2)} \right)$$

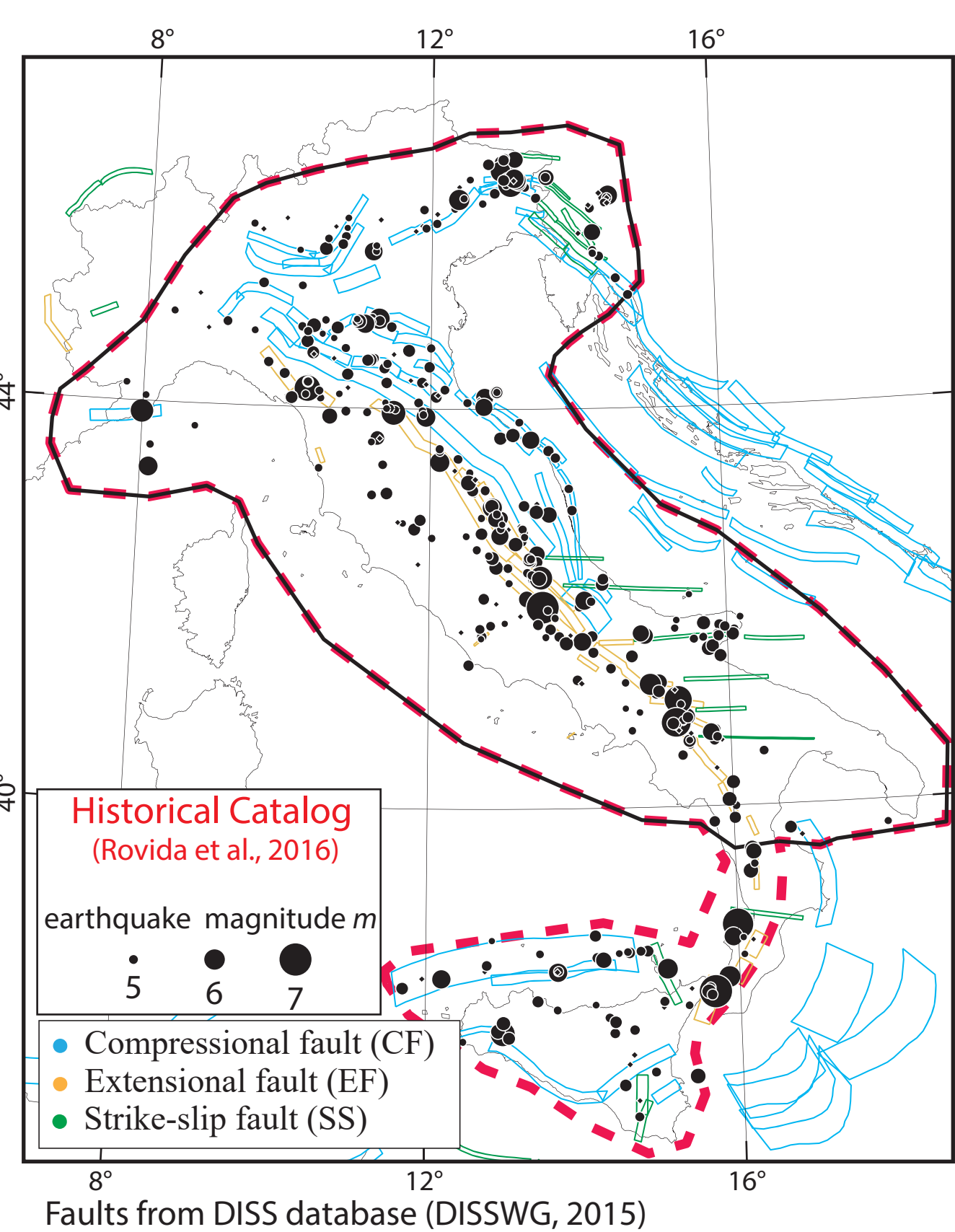
coming back to coupled thickness estimation...

$$\langle cz \rangle = \frac{\alpha_0(k) \cdot M_t^\beta \cdot \Gamma[2-\beta] \cdot M_c^{1-\beta} \cdot \exp[M_t/M_c]}{\mu \cdot A \cdot \left(\frac{\dot{\epsilon}_{med}}{\cos(\theta_1)\sin(\theta_1)} + \frac{\dot{\epsilon}_{least}}{\cos(\theta_2)\sin(\theta_2)} \right)}$$

still TO BE DETERMINED DETERMINED

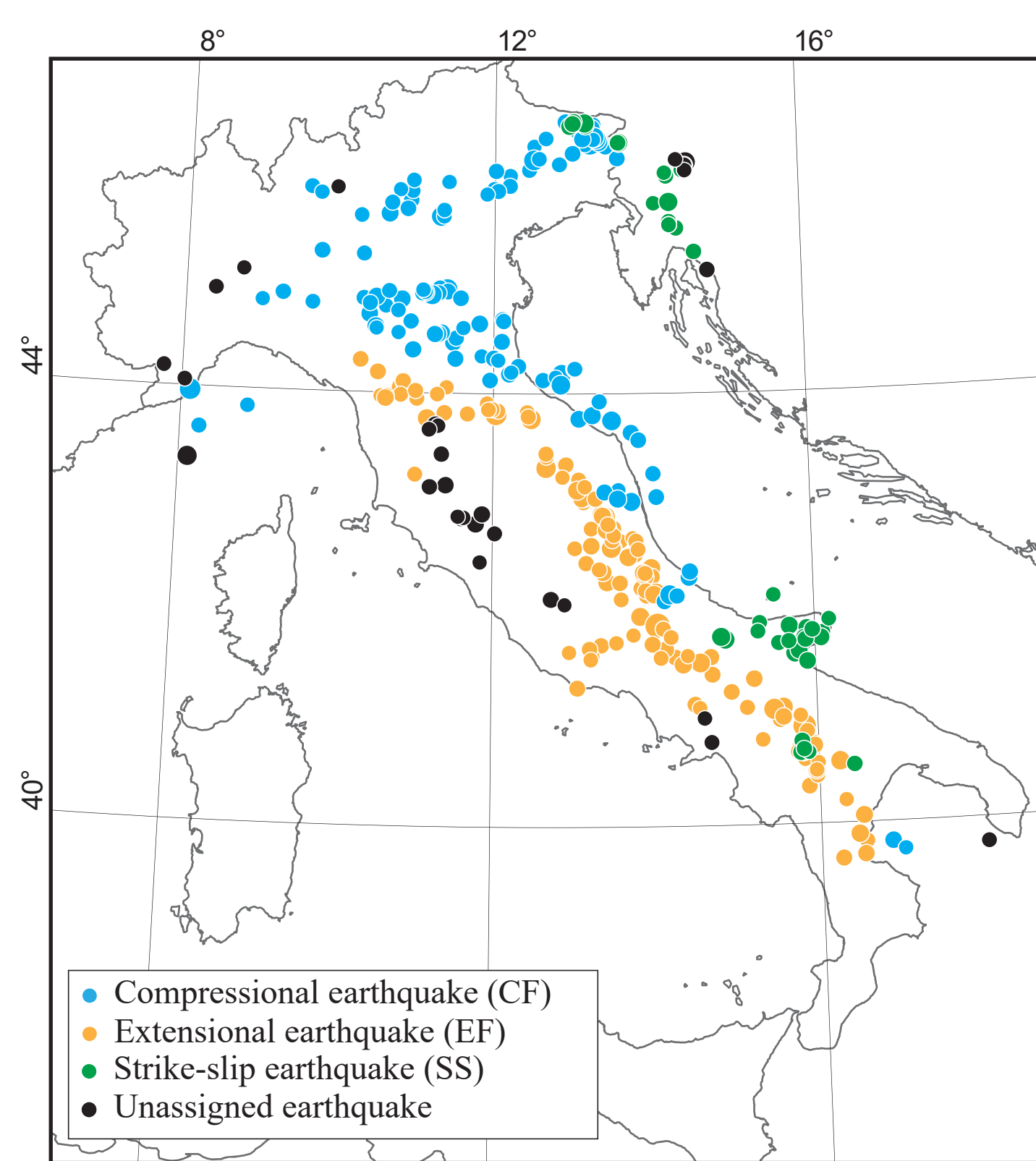


Assigning historical earthquakes to causative faults and determining α_0



Our method for assigning earthquakes from the historical catalog to DISS faults follows Bird & Kagan (2004) in its three-step method and Bayesian philosophy. In the first step, we make a prior assumption that a single earthquake has been generated by each DISS fault, in turn, and compute a set of maps of the probability densities that the epicenter has various possible locations near the fault trace. In the second step, we make a different prior assumption: that a particular historical earthquake was generated by one of these DISS faults. The ratios of probability densities computed in the first step are then scaled (also considering relative fault activity) to be absolute probabilities that each of the faults was the source. In a few cases where all probability densities are zero, we will reject the prior assumption, and the earthquake will remain unclassified. In those cases where we can proceed to the third step, we will assign the historical earthquake to the most likely causative fault, using either a maximum-probability criterion or a Monte-Carlo method, based on the absolute probabilities computed in step 2. Once the earthquake is assigned to a fault, it will take its tectonic class assignment (EF, CF, or SS) from the known rake of that fault.

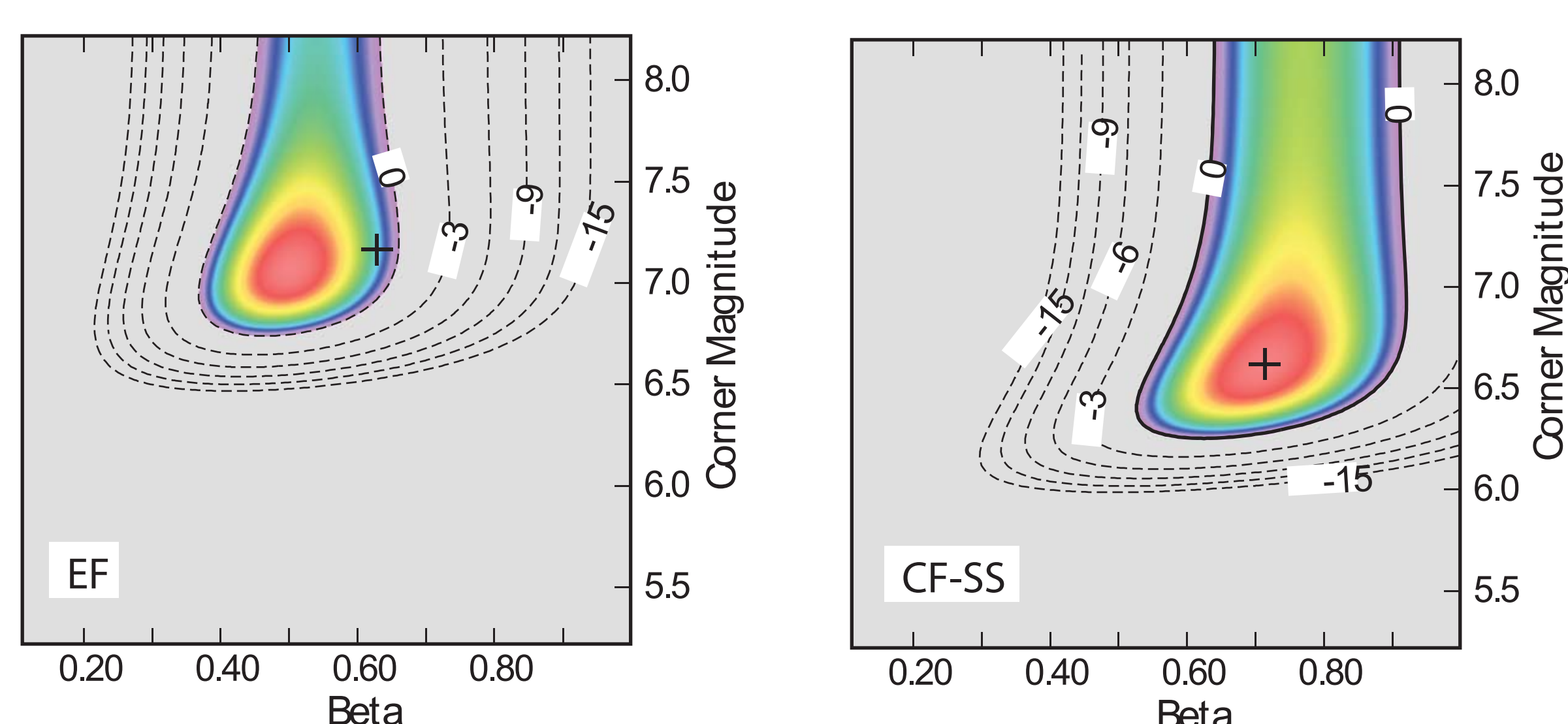
Unassigned earthquakes: 32 (reassigned proportionally)
Compressional Earthquakes $\alpha_0=134 (+13.7)$
Extensional Earthquakes $\alpha_0=140 (+14.3)$
Strike-slip Earthquakes: $\alpha_0=40 (+4.1)$



Determining β and M_c for each class

Once the three subcatalogues were populated we determined the maximum-likelihood estimates of β and M_c to calculate the coupled thickness. The number of earthquakes and their magnitude distribution for the SS subcatalogue, however, is insufficient to obtain a stable result; thus we dismissed this subcatalogue as unsuitable for β and M_c estimation.

The location of these faults in the DISS database, all Iy in the Adriatic foreland next to thrust faults, suggests that a common geological settings could result in similar values for Gutenberg-Richter parameters between these two classes. Based on this reasoning we merged the CF and SS subcatalogues for purposes of estimating their common Gutenberg-Richter parameters. This combined CF-SS subcatalogue is used only for the determination of β and M_c , whereas for seismic moment rate estimations the earthquakes in each subcatalogue are kept separate.



Seismicity parameters for shallow continental faults in Italy

	Subcatalogues based on fault kinematics		
	CF Compressional faults	EF Extensional Faults	SS Strike-slip Faults
Earthquakes from CPT115 1880-2013, $m=4.8$	147.7	154.3	44.1
Asymptotic slope β	$0.71_{-0.12}^{+0.14}$	$0.63_{-0.12}^{+0.14}$	$0.71_{-0.12}^{+0.14}$
Corner magnitude m_c	$6.62_{-0.3}^{+0.7}$	$7.17_{-0.35}^{+0.7}$	$6.62_{-0.3}^{+0.7}$
Seismic moment rate \dot{M}_{seis} , $N m/s \times 10^9$	$12.8_{-3.3}^{+7}$	$32.3_{-11.5}^{+7}$	$3.8_{-1.0}^{+7}$
Shear modulus μ , GPa	$35.2_{-6.0}^{+5.4}$	$35.2_{-6.0}^{+5.4}$	$35.2_{-6.0}^{+5.4}$
Average fault-to- z_{great} angles, $\theta_1 = \theta_2$, °	35	49	76
Coupled thickness cz , km	$3.7_{-1.4}^{+2}$	$7.2_{-3.3}^{+2}$	$4.8_{-1.9}^{+2}$

Some notes on the main role of geology in explaining results (thus in seismic hazard)

1. Coupled thickness and corner magnitude significantly differ between compressional faults and extensional faults in Italy

2. Coupled thickness is:
- notably higher than the corrsipective global analog for Extensional Faulting
- notably lower than the corrsipective global analog for Compressional Faulting

The thick evaporite formations encircling the Italian peninsula along the external margin of the Apennines chain are effective impermeable seals which control the escape of fluids from beneath, thus potentially increasing local fluid pressures. Once a subduction zone slows down or stops moving, as the Apennines arcs have done in the recent geological past, these super-hydrostatic pore pressures should leak away slowly, at least in principle, but we do not know how long this process takes. This high pore pressure in the forearc areas, like the Apennines (EF faults), reduces the shear stress necessary for frictional sliding. In addition to that, the Apennines (and in general the Mediterranean forearcs of subduction zones) exhibit an unusually low heat-flow (e.g., 35-60 mW/m2), comparable only to the least radiogenic parts of the old shields (Baltica, Laurentia). The combination of these high pore pressures, high strain rates and low temperatures is likely to cause the critical brittle/ductile transition depth (for any local rheology) and the related seismicity cutoff to be deeper than normal. From a rheological perspective the main consequence of these circumstances is that brittle deformation is encouraged to continue to greater depth because temperatures are still too low to deform the upper crust by ductile creep, and effective pressures are too low to impose plastic behavior.

References

Bird P. and M. M. C. Carafa (2016), Improving deformation models by discounting transient signals in geodetic data. I: Concept and synthetic examples, Journal of Geophysical Research: Solid Earth, 121, 5538–5556, doi:10.1002/2016JB013056.

Carafa, M.M.C. & Bird, P., 2016. Improving deformation models by discounting transient signals in geodetic data. 2. Geodetic data, stress directions, and long-term strain rates in Italy, Journal of Geophysical Research: Solid Earth, 121, 5557–5575, doi: 10.1002/2016jb013038.

Carafa, M. M. C., G. Valensise, and P. Bird (2017), Assessing the seismic coupling of shallow continental faults and its impact on seismic hazard estimates: a case-study from Italy, Geophys J Int, 209(1), 32–47, doi: 10.1093/gji/ggx002.

DISS Working Group (2015), Database of Individual Seismogenic Sources (DISS), Version 3.2.0: A compilation of potential sources for earthquakes larger than M 5.5 in Italy and surrounding areas. http://diSS.mi.ingv.it/diSS/, INGV; DOI:10.6092/INGV.IT-DISS3.2.0

Rovida A., Locati M., Camassi R., Lollì B., Gasperini P. (eds), 2016. CPT115, the 2015 version of the Parametric Catalogue of Italian Earthquakes. Istituto Nazionale di Geofisica e Vulcanologia. doi:http://doi.org/10.6092/INGV.IT-CPT115